

SUPPORTING INFORMATION

Quantifying acute fuel and respiration dependent pH homeostasis in live cells using the mCherryTYG mutant as a fluorescence lifetime sensor

Emily P. Haynes¹, Megha Rajendran^{1,2,†}, Chace K. Henning[‡], Abhipri Mishra[‡], Angeline M. Lyon^{1,3,4}, Mathew Tantama^{1,2,3*}

¹Department of Chemistry, ²Institute for Integrative Neuroscience, ³Institute of Inflammation, Immunology, and Infectious Disease, ⁴Department of Biological Sciences, Purdue University, 560 Oval Drive, Box 68, West Lafayette, IN 47907, USA

*CORRESPONDENCE: E-mail: mtantama@purdue.edu

CONTENTS

Supporting Methods

Figure S-1. Structural comparison of mCherryTYG, mCherry, and mOrange

Figure S-2. mCherryTYG characterization by steady-state fluorescence spectroscopy

Figure S-3. Maturation of red fluorescence.

Figure S-4. Fitted fluorescence lifetime decay components for protein and cell pH calibrations

Figure S-5. Live-cell spectroscopy for fuel and respiration dependent pH

Figure S-6. Non-binding ATeamYEMK mutant controls

Figure S-7. Two-color simultaneous measurement of fuel-dependent pH and ATP

Figure S-8. Two-color simultaneous measurement of intracellular and extracellular pH

Table S-1. Steady-state fluorescence properties of RFPs

Table S-2. Data collection and refinement statistics

Table S-3. Fitted fluorescence lifetime decay components for purified protein pH calibration.

Table S-4. Fitted fluorescence lifetime decay components for pH-clamped live *E. coli* calibration.

Supporting Methods

Molecular Biology. The wildtype mCherry gene was mutated to mCherryTYG using the NEB Q5 Mutagenesis kit (forward primer: ACCTACGGTTCCAAGGCCTACGTGAAG; reverse primer: GAACTGAGGGGACAGGATG) within the pRSETB bacterial expression vector or the GW1 mammalian expression vector. The mCherryTYG-mTurquoise2 fusion was constructed by linearizing the GW1-mCherryTYG plasmid with BsrGI, amplifying the mTurquoise2 gene by PCR (forward primer: AGTAAGAATTCGAAGCTTGTGATCATAATCAGCCATACACATT; reverse primer: AGCTCGTCCATGCCGC) to add compatible overlaps, and the NEB HiFi kit was used to insert mTurquoise2 on the C-terminal end of mCherryTYG via a Gibson reaction. mTurquoise2-N1 was a gift from Michael Davidson & Dorus Gadella (Addgene plasmid # 54843).

Protein Expression and Purification. The pRSETB-mCherryTYG plasmid was transformed into BL21(DE3) E. coli cells and grown in Autoinduction Media (Formedium) at 37 °C in baffled flasks with continuous shaking overnight for 12-16 hours followed by 2-3 days of continuous shaking at ambient temperatures. Cells were pelleted at 6,000xg and stored at -80 °C until purification. His-tagged protein was purified by nickel-affinity chromatography using a HiTrap IMAC column (Amersham) according to manufacturer instructions. Purified protein was dialyzed against storage buffer (5 mM MOPS, 300 mM NaCl, 10% glycerol, pH 7.3), concentrated to 500 uL using a 10,000 MWCO Amicon Centrifugal Filter (Millipore), and stored at -20 °C for immediate use or -80 °C for extended storage. Protein produced for crystallization was further polished by size-exclusion chromatography using tandem Superdex S200 columns (GE Healthcare) pre-equilibrated with 50 mM HEPES pH 7.9 (Shu et al 2006). Fractions containing mCherryTYG were pooled and concentrated to 20 mg/mL for crystallization.

Steady-State Fluorescence Spectroscopy. pH titrations were performed by diluting protein to 0.2 - 1 μ M in assay buffer containing 50 mM Tris, 50 mM Bis-Tris, 50 mM MOPS adjusted to pH 5.5 - 9.0 with NaOH or HCl at half unit steps. Fluorescence was measured on a microplate reader (Biotek synergy H5). Emission spectra were measured using a monochromator with fixed excitation at 540/9 nm and emission scanned from 560 – 700 nm with a 9 nm emission bandpass. Excitation spectra were measured using a monochromator with fixed emission at 600/9 nm and excitation scanned from 480 – 580 nm with a 9 nm excitation bandpass. To test for environmental interference, protein samples were prepared in assay buffer containing either 100mM NaCl, 100 mM KCl, 1 mM MgCl₂, 1mM CaCl₂, 10 μ M H₂O₂ or 30 μ M DTT. The concentration of protein containing mature chromophore was quantified by measuring absorbance of protein after alkaline denaturation in 1M NaOH at 450 nm (ϵ = 44000 M⁻¹·cm⁻¹) as previously described. Absorbance and fluorescence spectra of 5 - 20 μ M protein solutions at different pH were measured. Extinction coefficients were calculated according to the Beer-Lambert equation. Quantum yields were calculated from the slopes from integrated fluorescence (530 nm excitation) vs. absorbance relationships relative to the wildtype mCherry standard.

Mammalian Cell Culture, Transfection, and Live-Cell Imaging. HEK-293 cells were cultured at 37 °C in 5% CO₂ humidified air incubator in DMEM media containing 10% Cosmic calf serum (Hyclone). Cells were transfected using calcium phosphate and imaged after 2 days. Cells were imaged in high potassium imaging solution (mM: 1.25 NaH₂PO₄, 125 KCl, 2 CaCl₂, 1 MgCl₂, 10 glucose) containing 2.5 μ M nigericin and buffered to pH 5.5 to 9.0. The mCherryTYG fluorescence images were collected using 550/15 nm excitation, 570 nm longpass dichroic, and 585/20 nm emission filters. The mTurquoise2 fluorescence images were collected using 438/29 nm excitation, multiband dichroic, and 470/20 nm emission filters.

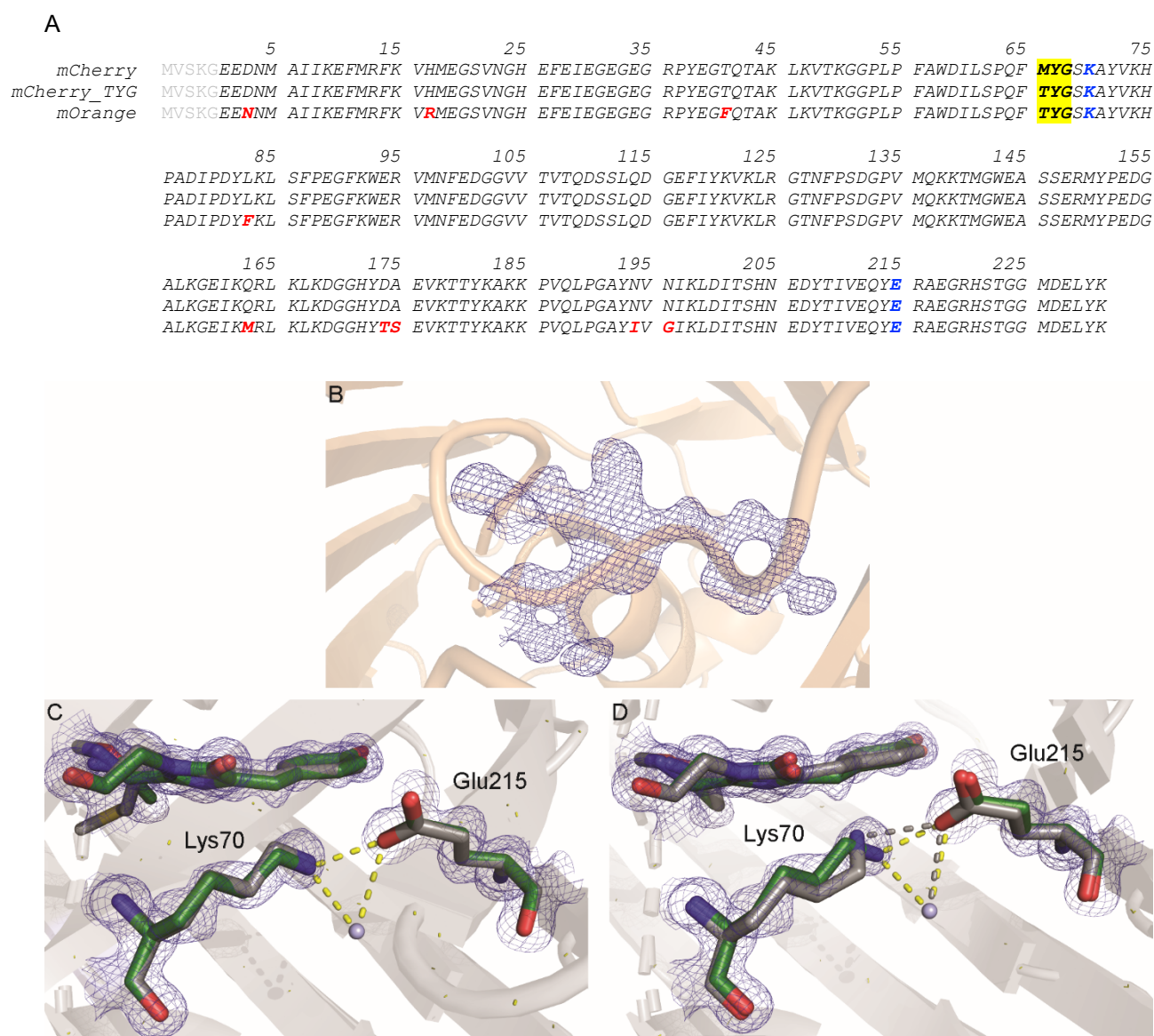


Figure S-1. Structural comparison between mCherryTYG, wildtype mCherry, and wildtype mOrange. (A) Protein sequence alignment for the different fluorescent proteins. Chromophore forming residues are highlighted in yellow. mOrange residues that differ from the mCherry scaffold are in bold red font. Conserved residues Glu215 and Lys70 are in bold blue font. (B) Omit map showing the electron density for the mCherryTYG chromophore. (C-D) In addition to Glu215, we also observed structural differences at Lys70. Lys70 is also thought to contribute to the local electric field around the chromophore, and in mCherryTYG residue Lys70 shows small deviations from its positions in wildtype mCherry and mOrange. In mOrange, the charged side chain of Lys70 hydrogen bonds to the same water coordination network interacting with Glu215. However, in mCherryTYG the electron density suggests the conformation of Lys70 more resembles the conformation in wildtype mCherry, and it does not interact with the water coordination sphere observed in mOrange. In mCherryTYG, Lys70 resembles the conformation found in wildtype mCherry (C) whereas mOrange exhibits a different rotamer for Lys70 (D). The mCherryTYG residues are colored green with overlays of (C) wildtype mCherry or (D) mOrange residues in grey.

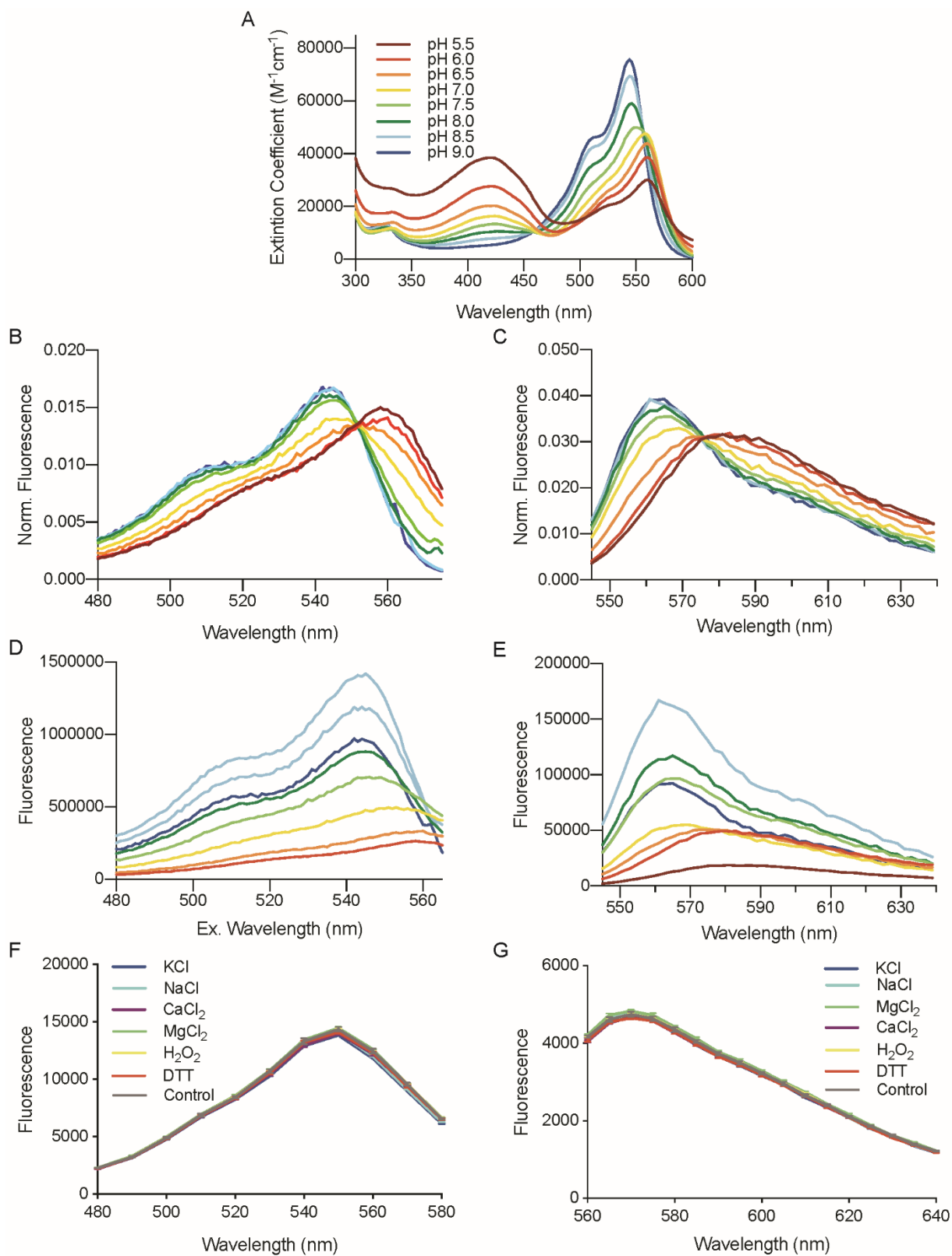


Figure S-2. Steady-state fluorescence spectroscopy characterization of mCherryTYG. The pH-dependent spectra were measured, including the (A) absorbance spectra, (B) raw fluorescence excitation spectra, (C) raw fluorescence emission spectra, (D) fluorescence excitation spectra normalized to total fluorescence, and (E) fluorescence emission spectra normalized to total fluorescence. The (F) fluorescence excitation and (G) emission spectra of mCherryTYG demonstrate that it is not sensitive to differences in physiological salts nor differences in redox environment.

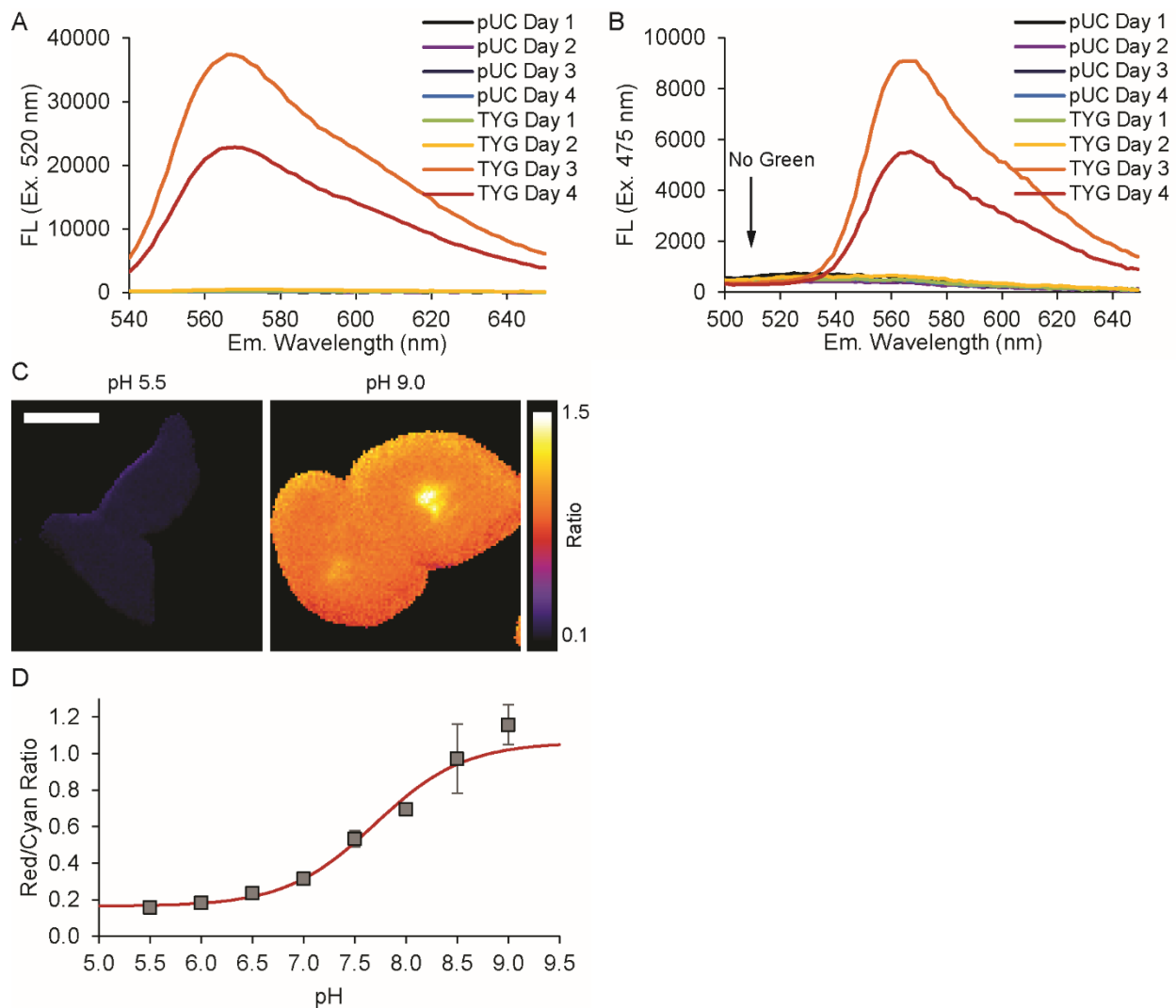


Figure S-3. mCherryTYG exhibits efficient maturation to the red fluorescent form. (A-B) Expression of mCherryTYG was monitored in live BL21(DE3) *E. coli*. (A) Emission spectra with 520 nm excitation were measured as direct excitation of the red chromophore as a reference. (B) To test if immature green fluorescent chromophore was present at any time point, emission spectra with 475 nm excitation were measured. Bleedthrough excitation of the fully mature red fluorescence chromophore was detected near 570 nm emission (note the 4-fold lower y-axis scale), but no green fluorescence near 510 nm emission was detected in mCherryTYG transformed cells relative to background measured in pUC transformed control cells. Similar results showing no detection of immature green fluorescent chromophore were obtained with DH5a *E. coli* ($n=3$ for each cell type and plasmid). (C-D) mCherryTYG mature efficiently and is well-behaved when expressed in mammalian cells. HEK293 cells expressing mCherryTYG did not show any evidence of immature green fluorescence. To demonstrate that mCherryTYG maintained pH sensing, we constructed the mCherryTYG-mTurquoise2 fusion as a ratiometric pH sensor. HEK293 cells expressing mCherryTYG-mTurquoise2 were incubated in high potassium imaging solution with the equilibrative H^+/K^+ nigericin and buffered at pH 5.5 to 9.0. The ratio of mCherryTYG red fluorescence intensity to mTurquoise2 cyan fluorescence intensity exhibits a pH dependent change with pK_a of 7.7 (mean \pm std).

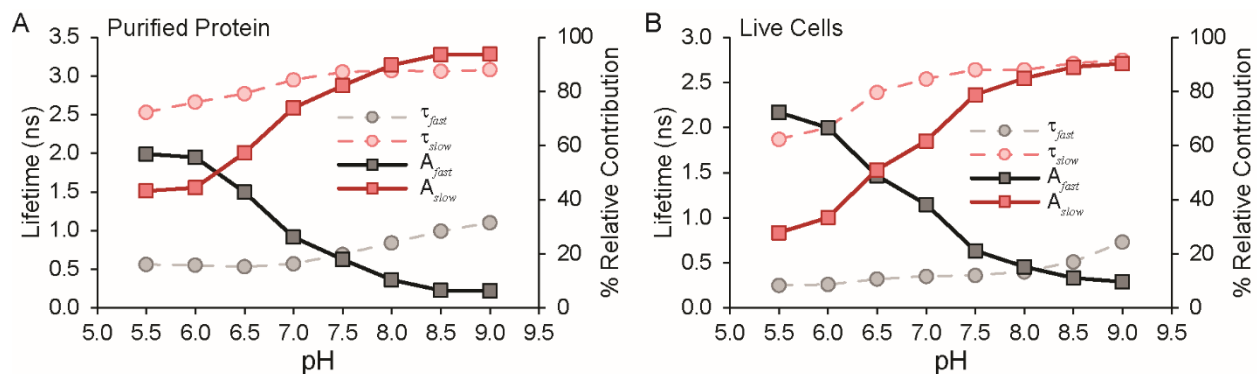


Figure S-4. Fluorescence lifetime decay time constants. Plots of the time constants obtained by reconvolution fitting for sample-matched IRFs also reported in Tables S1 and S2 for pH calibration curves obtained from (A) purified mCherryTYG protein or (B) mCherryTYG expressed in live *E. coli* with benzoate and methylamine pH clamping. The pH dose response of the relative amplitude of the slow component exhibits (A) a pK_a of 6.81 ± 0.08 for purified protein and (B) a pK_a of 6.7 ± 0.1 for live cells.

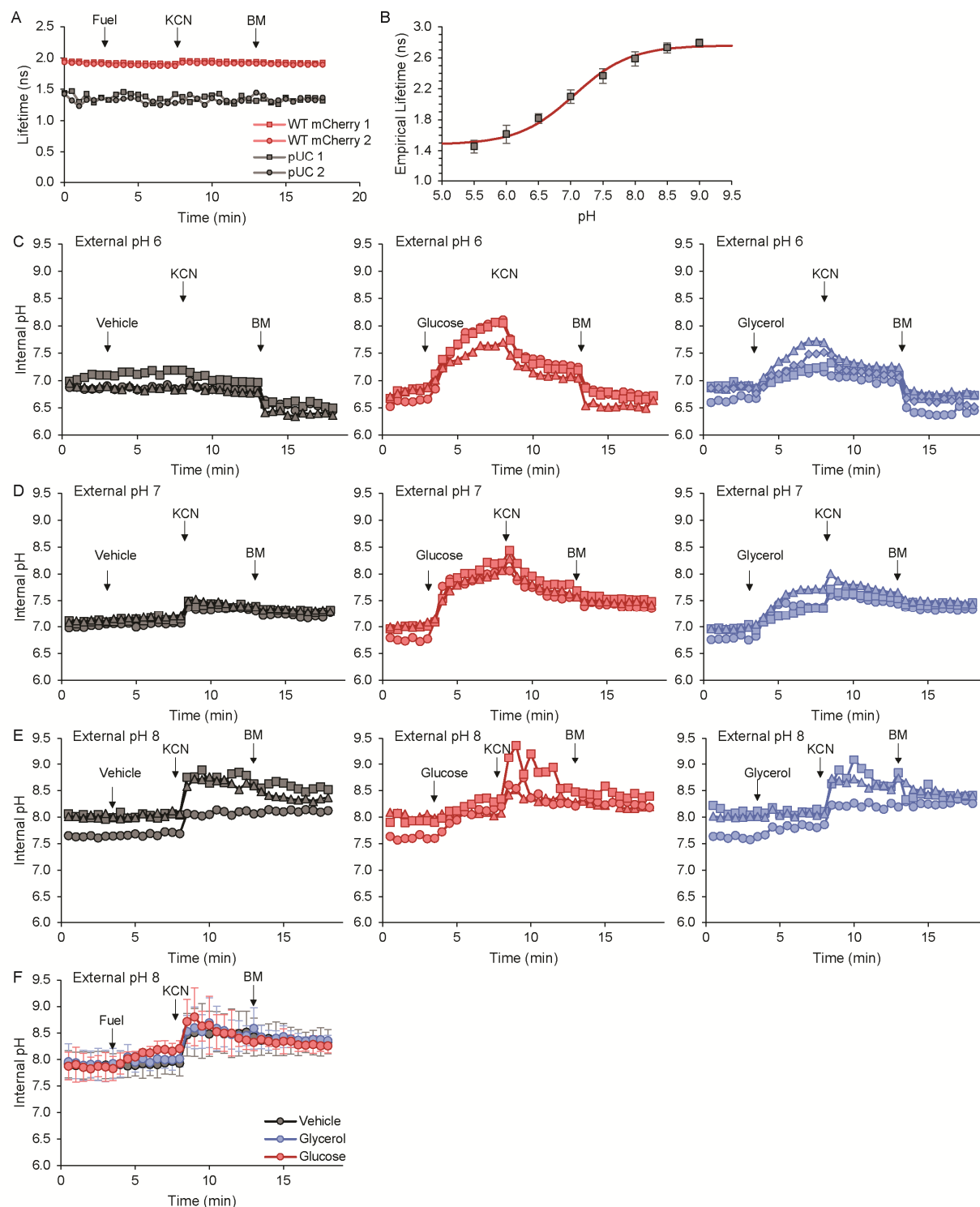


Figure S-5. Live-cell time-resolved spectroscopy on *E. coli* suspensions. (A) Controls using pUC cells expressing no fluorescent protein and cells expressing pH-insensitive wildtype mCherry show no change in lifetime with fuel or cyanide addition in M63 media at pH 6. (B) Calibration curve for the empirical tail mean lifetime for continuous live-cell assays. (C-E) Each trace is the pH response for an independent culture of mCherryTYG expressing cells in M63 media at (C) pH 6, (D) pH 7, and (E) pH 8. (F) The average response at pH 8 (mean \pm 95%CI) trended towards alkalinization only with the glucose addition.

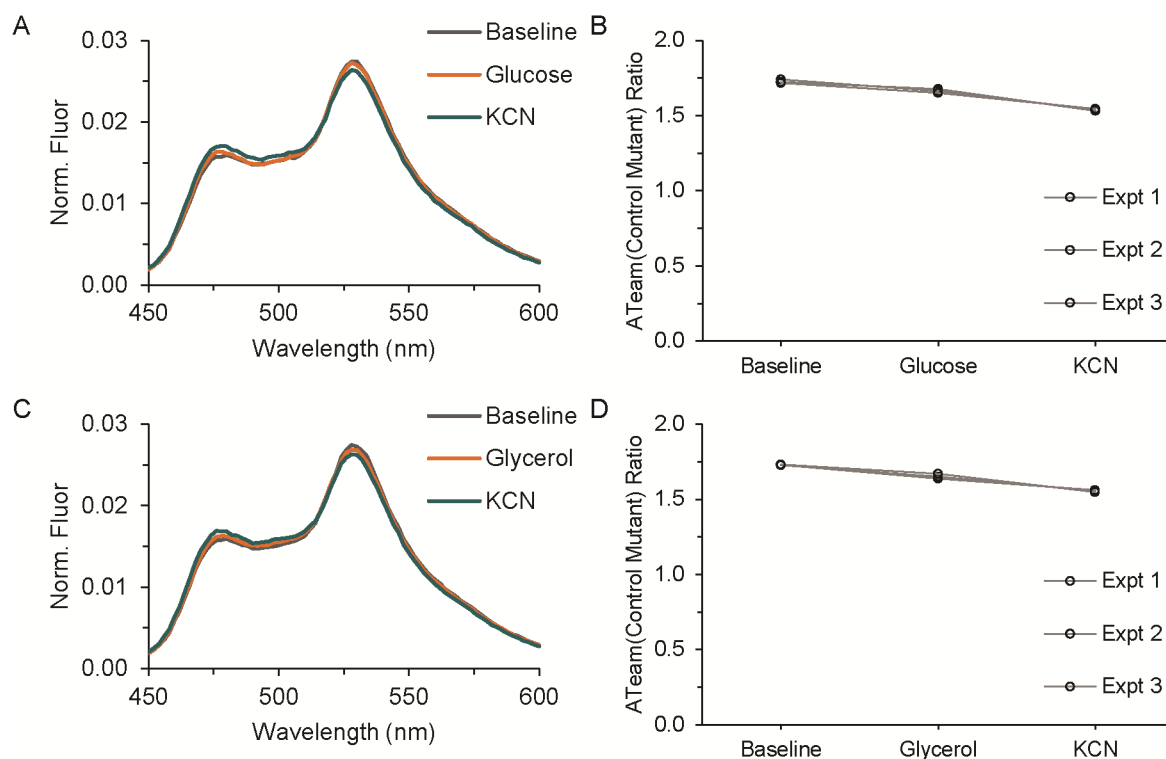


Figure S-6. Non-binding ATeamYEMK mutant controls. The ATeam sensor is known to be pH sensitive, but between pH 7.0 to 8.0 the ATeam sensor is far more sensitive to changes in ATP compared to pH (Imamura *et al.* 2009 PNAS). To validate that the ATeam sensor reports true changes in ATP and that the spectral changes are not an artifact of a pH change, we used live cells expressing the ATeam1.03YEMK(R103A) mutant that does not bind ATP. Neither glucose (A-B) nor glycerol (C-D) fuel addition causes a substantial change in the steady-state FRET/CFP emission ratio, and there is only a minor decrease in the ratio after the addition of KCN. The ratios values are: (A-B) baseline, 1.73 ± 0.01 ; glucose, 1.66 ± 0.01 ; KCN, 1.54 ± 0.01 ; (C-D) baseline, 1.73 ± 0.01 ; glycerol, 1.65 ± 0.02 ; KCN, 1.56 ± 0.01 ; mean \pm 95%CI. Thus, control experiments using live cells expressing the non-binding mutant demonstrate that the pH sensitivity of the ATeam sensor is minor under our conditions and does not account for the large ratio changes observed and reported in Figure 5.

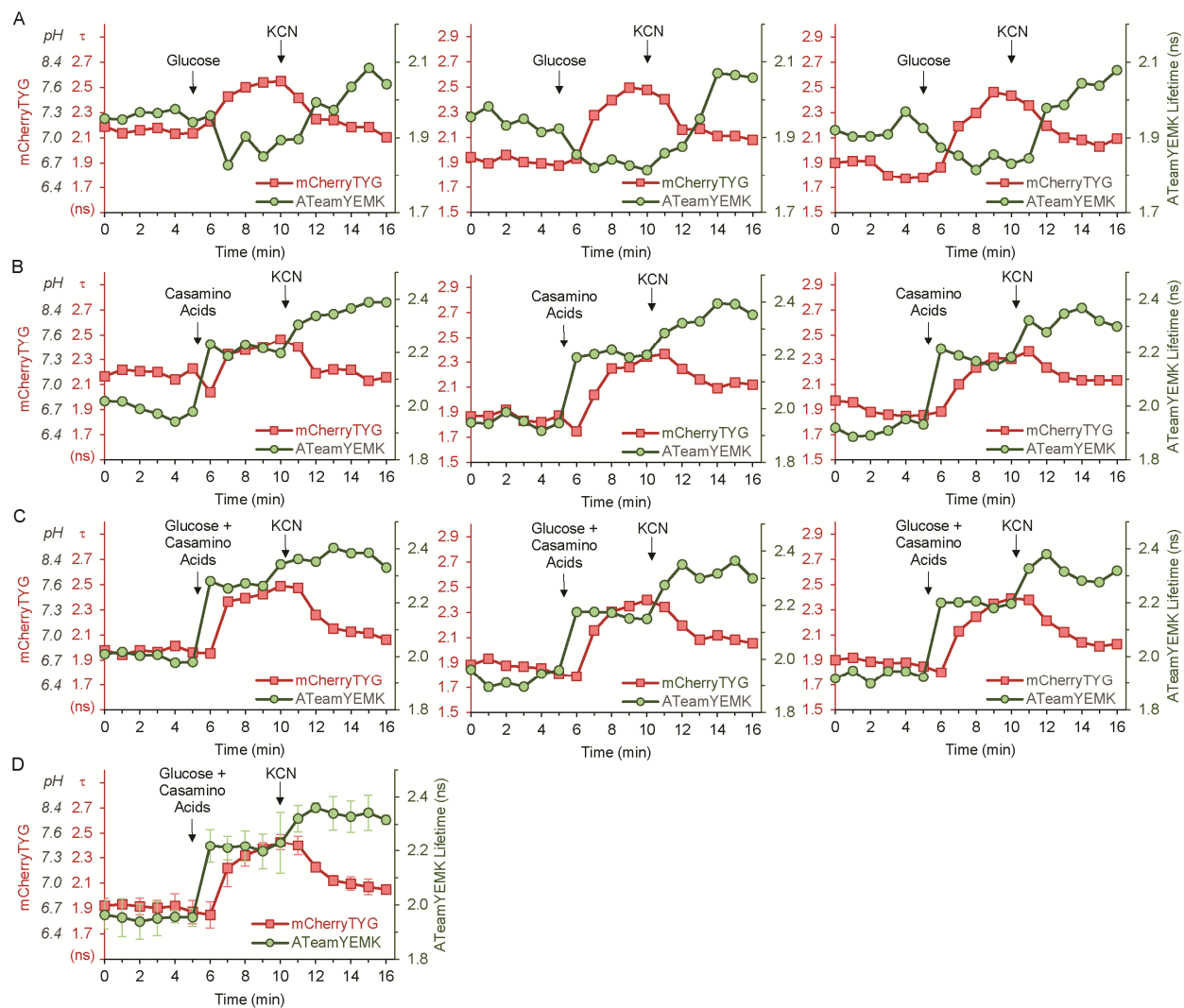


Figure S-7. Simultaneous two-color live-cell lifetime measurements directly correlate intracellular pH and ATP levels. Each plot shows the correlated mCherryTYG (red) and ATeamYEMK (green) individual time-course data for independent experiments testing the effects of (A) glucose addition, which is presented as averaged data in Figure 6A, and (B) glycerol addition, which is presented as averaged data in Figure 6B. (C-D) The addition of casamino acids together with glucose supports respiration and causes intracellular alkalinization reported by the increase in the mCherryTYG lifetime. However, casamino acid transport and metabolism consumes ATP and causes a decrease in intracellular ATP levels reported by the increase in ATeam donor lifetime, even in the presence of glucose. Individual time-course data for independent experiments (C) and averaged data (D) are presented.

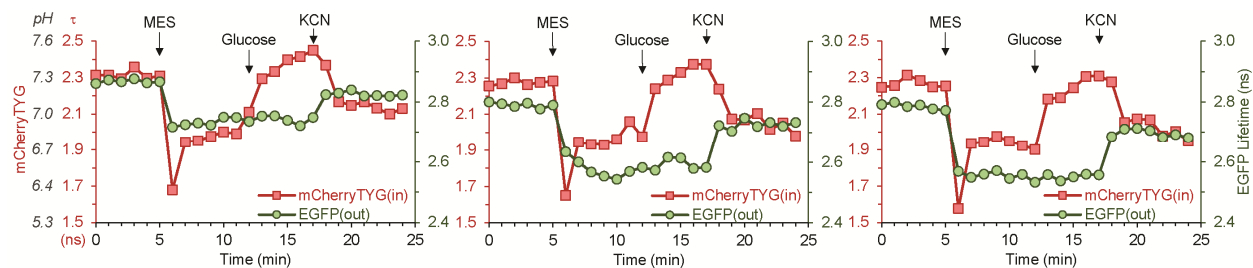


Figure S-8. Simultaneous two-color live-cell lifetime measurements directly correlate intracellular pH and extracellular pH. Each plot shows the correlated intracellular mCherryTYG (red) and extracellular EGFP (green) individual time-course data for independent experiments that are presented as averaged data in Figure 7.

Table S-1. Steady-state properties of fluorescent proteins.

RFP	Ex. (nm)	Em. (nm)	ϵ ($M^{-1}\cdot cm^{-1}$)	ϕ	pKa ⁴
mCherry-TYG ^{1,2} (pH 5.5) (pH 9.0)	558	582	20,000	0.05	7.4 ¹ ; 7.8 ²
	543	562	55,000	0.31	
mOrange ³	548	562	71,000	0.69	6.5
mCherry ³	587	610	72,000	0.22	4.5

¹ This study; ² Shen *et al.*; ³ Shaner *et al.*⁵³; ⁴ Steady-state pK_a calculated from pH-dependent change in fluorescence intensity brightness.

Table S-2. Data collection and refinement statistics

Data Collection	
X-ray source	LS-CAT 21-ID-D
Wavelength (Å)	1.088 Å
D _{min} (Å)	20.0– 1.09
Space group	<i>P</i> 12 ₁ 1
Cell dimensions	
a, b, c (Å)	48.8, 42.8, 61.1
α , β , γ (°)	90, 112.2, 90
Total reflections	473,526
Unique reflections	69,505
R _{sym} (%)	0.095 (0.072)
Completeness (%)	93.6 (100.0)
(<i>I</i> / σ)	10.4 (23.1)
Redundancy	6.8 (7.0)
(<i>CC</i> _{1/2})	0.996 (0.993)
Refinement	
Refinement resolution (Å)	20.0 – 1.09
Total reflections used	76,260
RMSD bond lengths (Å)	0.005
RMSD bond angles (°)	1.04
Estimated coordinate error (Å)	0.09
Ramachandran plot	
Favored (%)	98.6
Outliers (%)	0.0
R _{work} /R _{free} (%)	16.7/17.7
Protein atoms	2,168
Ligand atoms	22
Solvent molecules	313
Average B-factor (Å ²)	15.9
Protein	14.3
Ligand	16.6
Solvent	25.3
Wilson B factor (Å ²)	11.7
PDB entry	6M3Z

Table S-3. Fitted fluorescence lifetime decay components for the purified protein pH calibration (mean \pm std).

pH	τ_{fast} (ns)	Rel.%	τ_{slow} (ns)	Rel.%	τ (ns)	χ^2
5.5	0.56 ± 0.01	57.7 ± 0.8	2.56 ± 0.03	42.3 ± 0.8	1.40 ± 0.01	1.11 ± 0.05
6.0	0.54 ± 0.01	55 ± 1	2.64 ± 0.02	45 ± 1	1.48 ± 0.02	1.17 ± 0.02
6.5	0.55 ± 0.02	44 ± 2	2.81 ± 0.04	56 ± 2	1.81 ± 0.01	1.2 ± 0.1
7.0	0.58 ± 0.01	26.6 ± 0.5	2.98 ± 0.03	73.4 ± 0.5	2.34 ± 0.02	1.11 ± 0.05
7.5	0.68 ± 0.01	17.8 ± 0.1	3.06 ± 0.02	82.2 ± 0.1	2.64 ± 0.02	1.08 ± 0.03
8.0	0.85 ± 0.02	10.6 ± 0.5	3.09 ± 0.03	89.4 ± 0.5	2.86 ± 0.03	1.09 ± 0.05
8.5	1.09 ± 0.09	7.1 ± 0.8	3.11 ± 0.05	92.9 ± 0.8	2.96 ± 0.04	1.11 ± 0.04
9.0	1.26 ± 0.14	8 ± 1	3.10 ± 0.02	92 ± 1	2.96 ± 0.01	1.13 ± 0.04

Table S-4. Fitted fluorescence lifetime decay components for the pH-clamped live *E. coli* calibration (mean \pm std).

pH	τ_{fast} (ns)	Rel.%	τ_{slow} (ns)	Rel.%	τ (ns)	χ^2
5.5	0.29 ± 0.03	67 ± 5	1.87 ± 0.05	33 ± 5	0.8 ± 0.1	1.63 ± 0.06
6.0	0.31 ± 0.04	62 ± 4	2.04 ± 0.04	38 ± 4	1.0 ± 0.1	1.6 ± 0.1
6.5	0.35 ± 0.03	45 ± 3	2.39 ± 0.01	55 ± 3	1.47 ± 0.08	1.36 ± 0.05
7.0	0.38 ± 0.03	35 ± 3	2.53 ± 0.02	65 ± 3	1.79 ± 0.08	1.26 ± 0.09
7.5	0.46 ± 0.09	18 ± 3	2.67 ± 0.03	82 ± 3	2.3 ± 0.1	1.17 ± 0.08
8.0	0.5 ± 0.1	13 ± 2	2.69 ± 0.05	87 ± 2	2.4 ± 0.1	1.14 ± 0.04
8.5	0.6 ± 0.1	9 ± 2	2.73 ± 0.03	91 ± 2	2.54 ± 0.06	1.1 ± 0.1
9.0	0.7 ± 0.2	8 ± 2	2.75 ± 0.03	92 ± 2	2.58 ± 0.04	1.14 ± 0.01